

Efficient second-harmonic generation in birefringently phase-matched GaAs/Al₂O₃ waveguides

K. Moutzouris, S. Venugopal Rao, and M. Ebrahimzadeh

School of Physics and Astronomy, University of St. Andrews, North Haugh, Fife KY16 9SS, Scotland, UK

A. De Rossi, V. Berger, M. Calligaro, and V. Ortiz

THALES, Laboratoire Central de Recherches, Domaine de Corbeville, 91400 Orsay, France

Received June 18, 2001

We report efficient second-harmonic generation of femtosecond pulses in birefringently phase-matched GaAs/Al₂O₃ waveguides pumped at 2.01 μm . By use of pump pulses of ~ 200 -fs duration and type I interaction, practical second-harmonic average powers of up to ~ 650 μW were obtained, with an average input power of ~ 50 mW. Waveguides of four different widths and two different lengths were investigated, and a normalized conversion efficiency of greater than 1000% $\text{W}^{-1} \text{cm}^{-2}$ was obtained for a 1-mm waveguide. Measurements of pump and second-harmonic spectra provided clear evidence of phase matching and depletion of the pump spectrum. The measured bandwidth of the second harmonic was ~ 1.3 nm. From the measurements of transmitted pump power at the phase-matching wavelength, pump depletions of more than 80% were recorded. © 2001 Optical Society of America

OCIS codes: 190.5970, 190.2620, 160.4330, 230.7370.

Since the first experimental demonstration of birefringent phase matching by use of isotropic GaAs,¹ there has been considerable interest in this class of materials for potential applications in various functional devices, ranging from second-harmonic generation (SHG) structures to integrated devices for difference frequency generation, all-semiconductor optical parametric oscillators (OPOs), optical communications, and all-optical signal processing.^{2,3} Large second-order nonlinear coefficients, a broad range of mid-IR transparency, and the possibility of integration with semiconductor laser sources in a monolithic ensemble make GaAs-based devices attractive, especially for optical frequency-conversion applications in the mid-IR, where compact and efficient laser sources are sparse. Other distinct advantages of GaAs over existing materials include room-temperature operation, mature growth and fabrication technology, and the potential for mass production and low cost. Because of a lack of intrinsic birefringence, phase matching in GaAs-based waveguide structures has been achieved with quasi-phase matching⁴⁻⁶ (QPM) or birefringent phase matching through selective oxidation of AlAs in AlGaAs/AlAs multilayers to form AlGaAs/Alox (aluminium oxide).^{1,7} Although QPM is attractive, the high scattering losses at present limit the useful interaction length of these waveguides and thereby the overall conversion efficiency. Based on birefringent phase matching, several second-order processes including SHG,⁸ difference frequency generation,^{9,10} and parametric fluorescence¹¹ have been successfully demonstrated in GaAs-based waveguides. In this Letter we report the generation of practical second-harmonic powers at high efficiency in birefringent GaAs/GaAlAs waveguides pumped with femtosecond pulses at 2.01 μm . The use of femtosecond pulses for frequency conversion is attractive because it offers the potential for use of GaAs-based waveguides in wavelength- and time-division multiplexing applications for optical telecommunications. To our knowledge, this

is the first report of nonlinear frequency conversion in birefringent GaAs/GaAlAs waveguides by use of femtosecond pulses.

Figure 1 shows the basic structure of the waveguide used for the SHG experiments. It consists of GaAs $\langle 001 \rangle$ substrate nonintentionally doped/1000-nm Al_{0.92}Ga_{0.08}As/1000-nm Al_{0.7}Ga_{0.3}As/ $4 \times (50\text{-nm AlAs}/250\text{-nm GaAs})/50\text{-nm AlAs}/1000\text{-nm Al}_{0.7}\text{Ga}_{0.3}\text{As}/30\text{-nm GaAs}$. The two 1- μm -thick AlGaAs layers first grown on the high-index substrate are cladding layers for optical confinement. A 2- μm -thick Al_{0.92}Ga_{0.08}As layer would be more efficient but fragile. For this reason, a two-layer cladding with one Al_{0.7}Ga_{0.3}As layer is used. The alloy composition and the layer thickness were designed so that the SHG wavelength would be phase matched near 1.0 μm . We first etched the waveguide ridges along the $\langle 110 \rangle$ direction to exploit the nonzero component of the nonlinear susceptibility tensor $\chi_{xyz}^{(2)}$. Then, mesas were also etched, permitting lateral oxidation of all 50-nm-thick AlAs layers. Typical losses of

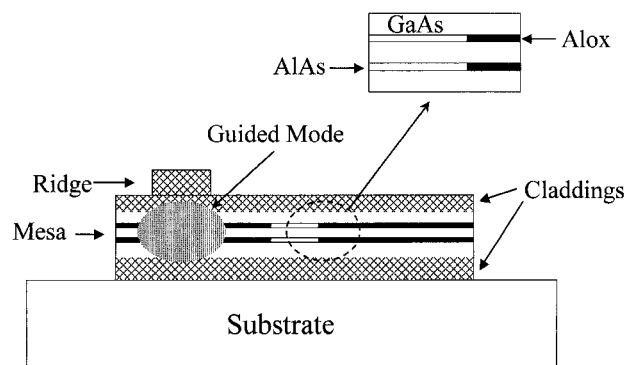


Fig. 1. Structure of the GaAs/Alox waveguide used in the SHG experiment. The position of the optical mode, overlapping with Alox layers, is shown schematically. The magnified part shows the oxidation front between AlAs and Alox.

$\sim 1 \text{ cm}^{-1}$ were measured in these waveguides at $1.32 \text{ }\mu\text{m}$. The strong refractive-index contrast between the semiconductor ($n \sim 3.4$) and Alox ($n \sim 1.6$) results in form birefringence strong enough to phase match the SHG process. Two samples of different lengths (1 and 2.2 mm), each with several waveguides of four different widths, were investigated.

The pump source was a synchronously pumped, singly resonant, femtosecond OPO based on periodically poled LiNbO_3 . Configuring the OPO in a semimonolithic cavity design permitted maximum extraction of the idler power,¹² which was used as the source of input pump pulses. A Kerr-lens mode-locked Ti:sapphire laser, operating near 820 nm and providing pulses of ~ 150 -fs duration at a 90-MHz repetition rate, pumped the OPO. The idler (here-with referred to as the pump) pulses from the OPO had a duration of ~ 200 fs ($\Delta\tau\Delta\nu \sim 0.38$, indicating that the pulses are nearly transform limited) and were tunable over a range 1.8–2.1 μm at an average power of ~ 50 mW. An end-fire coupling rig was used for mounting the sample. A half-wave plate placed in the beam path was used to control the polarization state of the pump idler beam. The TE-polarized pump pulses from the OPO were focused into the waveguide by a $40\times$ microscope objective. The transmitted SHG and the pump were collected by use of a second microscope objective ($20\times$). An IR camera was used to optimize the coupled pump into the waveguide. A germanium filter placed before the input objective cut any unwanted residual signals below $1.5 \text{ }\mu\text{m}$. We used a polarizing beam splitter at the output to separate out the TE pump and the TM second-harmonic signal. The transmitted pump power was measured with a calibrated InAs detector (sensitive in the 0.5–3.0- μm range) and a lock-in amplifier combination. A long-pass quartz filter ($T < 1\%$ for $\lambda \leq 1.6 \text{ }\mu\text{m}$) placed before the InAs detector ensured the exact measurement of only the transmitted pump power. The second-harmonic power was measured with a semiconductor-head powermeter.

Figure 2 shows the variation of the generated SHG average power with the square of pump power. As expected, the SHG power has a quadratic dependence on the input power. Figure 3 shows the typical spectra of the pump and SHG for a 1-mm-long waveguide. As is evident in Fig. 3(a), the input pump has a FWHM bandwidth of ~ 26 nm. The corresponding FWHM spectral width of SHG, shown in Fig. 3(b), is ~ 1.3 nm, indicating that only a part of the total pump bandwidth was utilized in the conversion process. That this is so is clearly verified by the incomplete spectral depletion of the transmitted pump, also shown in Fig. 3(b). For a 2.2-mm waveguide the FWHM bandwidth of SHG was ~ 0.95 nm. The spectral characteristics shown in Fig. 3 were typical of most of the waveguides in the sample. Figure 4 shows the second-harmonic power versus the central pump wavelength for a 1-mm waveguide. One can clearly see a phase-matching peak at $2.01 \text{ }\mu\text{m}$ for most of the waveguides, corresponding to $\text{TE}_0 \rightarrow \text{TM}_0$ interaction. The FWHM bandwidth of this peak was ~ 35 nm, which is larger than the spectral linewidth of the

pump (~ 26 nm). This FWHM bandwidth is related to the group-velocity mismatch and strong depletion of the pump.

To estimate the external efficiency ($P_{\text{SHG}}/P_{\text{PUMP}}$) of the process we measured the generated SHG power directly, using the semiconductor-head powermeter. For a 1-mm waveguide, the maximum usable SHG power measured after the output objective was $\sim 650 \text{ }\mu\text{W}$ for a pump power of 50 mW measured before the input objective. This maximum power represents an overall external efficiency of 1.3%. For a 2.2-mm waveguide it was 0.78% (390 μW of SHG power). Taking into account the losses from the microscope objectives, waveguide transmission, and facet reflectivities, we found that the internal conversion efficiencies are significantly higher. This conclusion

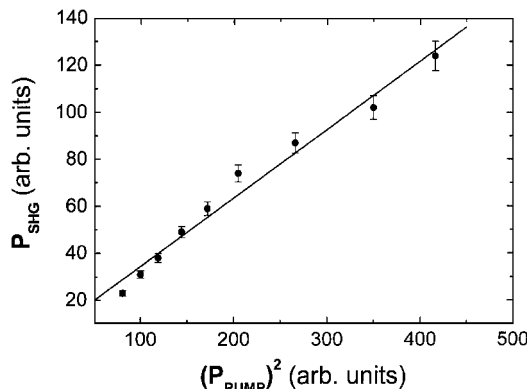


Fig. 2. Measured second-harmonic power plotted as a function of square of the pump power for a 1-mm waveguide.

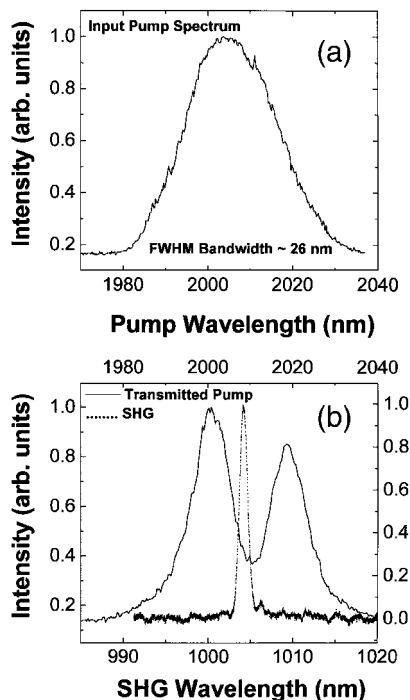


Fig. 3. (a) Pump spectrum with a FWHM bandwidth of ~ 26 nm. (b) Solid curve, transmitted, on-resonance depleted pump spectrum; dotted curve, corresponding second-harmonic spectrum (FWHM bandwidth, ~ 1.3 nm) for a 1-mm waveguide.

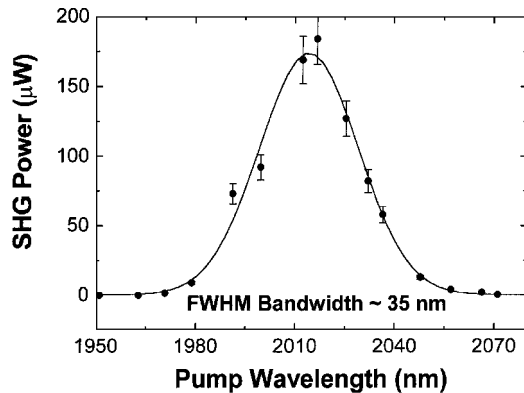


Fig. 4. Second-harmonic power plotted as a function of the input pump wavelength for a 1-mm waveguide. The FWHM bandwidth of this curve is ~ 35 nm.

is supported by our pump-depletion measurements, in which the transmitted pump power was recorded on and off resonance by use of an InAs detector and lock-in amplifier combination. We observed that, on resonance, typically 30–40% of the pump coupled into the waveguide was depleted (converted into SHG and other loss processes). The validity of pump-depletion measurements was also established through measurements of on- and off-resonance transmitted pump spectra by use of a highly sensitive monochromator. Although the off-resonance transmitted spectrum was smooth and Gaussian-like, there was a strong dip in on-resonance spectrum, clearly indicating the depletion of the input pump, as can be seen from Fig. 3(b). Within the conversion bandwidth, the depletion of pump was in fact greater than 80%. We also established that any spectral shift within the pump bandwidth resulted in no shift in the position of the dip in the transmitted pump spectrum or in the position of the peak in the SHG spectrum. These measurements were clear confirmation that the SHG process was indeed phase matched.

Accounting for the losses from the input microscope objective, the waveguide facet reflectivity ($\sim 30\%$), and a geometrical coupling factor (due to the difference in shape of the field outside and modal wave function inside the waveguide), we estimate that 5 mW of the pump power was coupled into the waveguide (for an available input power of 50 mW). Moreover, the detection efficiency at the output of the waveguide was lower than 50%. Considerations of group-velocity mismatch led to an estimate of the effective interaction length shorter than 200 μm . Taking into account the duty cycle (1.8×10^{-5}), we found that this results in a normalized conversion efficiency¹⁰ of greater than $500\% \text{ W}^{-1} \text{ cm}^{-2}$. Moreover, given that no more than one half of the pump spectrum is utilized in the conversion process, this corresponds to a waveguide-conversion efficiency of greater than $1000\% \text{ W}^{-1} \text{ cm}^{-2}$. This represents an increase of over 2 orders of magnitude from the previously reported value.⁸ However, with femtosecond pulses as were used here, the effects of group-velocity dispersion (and possible higher-order

nonlinear effects such as self-phase modulation and multiphoton absorption) also have to be considered before an accurate calculation of internal conversion efficiencies can be made. We are evaluating the exact theoretical limits of the generated SHG power and efficiencies in such waveguides, using femtosecond pulses.

In conclusion, we have demonstrated efficient SHG in type I birefringently phase-matched GaAs/Al_xO_y waveguides, using femtosecond pulses at 2.01 μm . Practical average SHG powers of $\sim 650 \mu\text{W}$, with an overall external efficiency of $\sim 1.3\%$ and a corresponding normalized waveguide efficiency of greater than $1000\% \text{ W}^{-1} \text{ cm}^{-2}$, were obtained, with an input pump average power of ~ 50 mW. We achieved depletion of as much as 40% in transmitted pump power, with more than 80% spectral depletion in the converted pump bandwidth. Extension of these experiments to the 1.2–1.6- μm wavelength band will allow the possibility for development of a new class of integrated devices for telecommunications applications based on GaAs technology.

This work was carried out under the EU European Strategic Programme for R&D in Information Technology project Optical Frequency Conversion in Semiconductors II. M. Ebrahimzadeh acknowledges the support of the Royal Society of London through a University Research Fellowship. His e-mail address is me@st-and.ac.uk; S. V. Rao's e-mail address is vrs2@st-and.ac.uk.

References

1. A. Fiore, V. Berger, E. Rosencher, P. Bravetti, and J. Nagle, *Nature* **391**, 463 (1998).
2. J. S. Aitchison, M. W. Street, N. D. Whitbread, D. C. Hutchings, J. H. Marsh, G. T. Kennedy, and W. Sibbett, *IEEE J. Sel. Top. Quantum Electron.* **4**, 695 (1998).
3. J. B. Khurgin, E. Rosencher, and Y. J. Ding, *J. Opt. Soc. Am. B* **15**, 1726 (1998).
4. S. J. B. Yoo, R. Bhat, C. Caneau, and M. A. Koza, *Appl. Phys. Lett.* **66**, 3410 (1995).
5. A. Saher Helmy, D. C. Hutchings, T. C. Kleckner, J. H. Marsh, A. C. Bryce, J. M. Arnold, C. R. Stanley, J. S. Aitchison, C. T. A. Brown, K. Moutzouris, and M. Ebrahimzadeh, *Opt. Lett.* **25**, 1370 (2000).
6. J. P. Bouchard, M. Tetu, S. Janz, D.-X. Xu, Z. R. Wasilewski, P. Piva, U. G. Akano, and I. V. Mitchell, *Appl. Phys. Lett.* **77**, 4247 (2000).
7. A. Fiore, V. Berger, E. Rosencher, N. Laurent, S. Theilmann, N. Vojdani, and J. Nagle, *Appl. Phys. Lett.* **68**, 1320 (1996).
8. A. Fiore, S. Janz, L. Delobel, P. van der Meer, P. Bravetti, V. Berger, E. Rosencher, and J. Nagle, *Appl. Phys. Lett.* **72**, 2942 (1998).
9. A. Fiore, V. Berger, E. Rosencher, P. Bravetti, N. Laurent, and J. Nagle, *Appl. Phys. Lett.* **71**, 3622 (1997).
10. P. Bravetti, A. Fiore, V. Berger, E. Rosencher, J. Nagle, and O. Gauthier-Lafaye, *Opt. Lett.* **23**, 331 (1998).
11. G. Leo, V. Berger, C. Ouyang, and J. Nagle, *J. Opt. Soc. Am. B* **16**, 1597 (1999).
12. P. J. Phillips, S. Das, and M. Ebrahimzadeh, *Appl. Phys. Lett.* **77**, 469 (2001).